THE BELL SYSTEM TECHNICAL JOURNAL
Vol. 59, No. 10, December 1980
Printed in U.S.A.

Sensitivity Loss of Digital Optical Receivers Caused by Intersymbol Interference

By F. S. CHEN and Y. S. CHEN

(Manuscript received July 24, 1980)

This paper describes studies of the dependence of optical receiver sensitivity on the launched-pulse width, pulse rise and fall times, and fiber dispersion for nonequalizing receivers. For pulse widths less than a time slot T in the return-to-zero (RZ) format and for small fiber dispersion σ_f, it is shown that the receiver sensitivity depends principally on the number of photons received per time slot and only weakly on the pulse width and rise and fall times of the launched pulses. For pulse widths equal to or greater than a time slot and/or with increased fiber dispersion ($\sigma_f/T > 0.2$), the receiver sensitivity degrades rapidly. Thus the sensitivity of receivers improves by use of reduced-width launched pulses in RZ format, particularly if the fiber dispersion is large. For example, for a receiver with equal thermal-noise and shot-noise levels, a situation approximating the use of an avalanche photodiode, the measured peak-power sensitivity penalty increased 2.5 dB as the launched-pulse width was increased from 0.6T to 1.1T for $\sigma_f/T = 0.4$. Since the peak-power sensitivity penalty has a broad minimum for pulse width between 0.5T to 1.0T, the use of reduced-width pulses in RZ format is also advantageous if the pulse width varies with temperature or varies among transmitters due to product variations.

I. INTRODUCTION

In a binary digital transmission system, the receiver sensitivity is degraded if received data pulses spread into neighboring time slots causing intersymbol interference (ISI). For an equalizing receiver design, as the received pulse width increases, the bandwidth of the equalizing network would have to be increased accordingly to minimize ISI at the output of the linear channel where the digital decision is made. As a result of the larger effective bandwidth, the noise input to the receiver increases. Therefore, more optical input power is required

to maintain the same bit error rate (BER); i.e., the sensitivity is reduced. For a nonequalizing receiver design, as the received pulse width increases, the eye of the output is allowed to close. To compensate for this eye degradation, more optical input power is required to achieve the same BER; i.e., the sensitivity is again reduced. Personick has analyzed the magnitudes of these sensitivity penalties arising from ISI in optical fiber transmission systems.[1,2] He concluded that no significant difference exists between equalizing and nonequalizing approaches, and nonequalizing receivers are easier and more practical to implement since they do not require a prior knowledge of the fiber dispersion. In his analysis, the input pulse width was set equal to one full time slot (non-return-to-zero, or NRZ, format), and the sensitivity penalty arising from fiber dispersion was then calculated.[2] A similar analysis for reduced-width, return-to-zero (RZ) pulses, which were subsequently broadened by fiber dispersion, was reported by Smith and Garrett[3] for equalizing receivers. They showed that, for cases where fiber bandwidth was a significant limitation, the sensitivity penalty could be decreased by launching reduced-width pulses into the fiber. An often encountered question, however, is what would the sensitivity penalty be for a practical nonequalizing receiver with launched pulses, having given variations in width and rise-fall times, and a given magnitude of fiber dispersion? Variations in width and transition times of launched pulse can arise from practical considerations of the transmitter performance and product spread. Depending on the optical source and the driver circuit, the width and transition times of output pulses from light emitters can deviate from those of the electrical signal at the input to the driver circuit. For example, the deviation in pulse width can be caused by the finite time it takes to turn on the light emitter and/or a difference between the leading- and trailing-edge propagation delay times in the driver circuit. Moreover, the magnitude of these deviations can vary with ambient temperatures. With a knowledge of sensitivity penalties, proper tradeoffs among the designs of various components in a fiber transmission system can be made.

In this paper, we present an analys compare these with measured receiver sensitivity. We function of launched-pulse width and fiber dispersion for nonequalizing receivers, and compare these with measured receiver sensitivity. We also present the results of experiments in which rise and fall times as well as the widths of launched pulses are varied, a situation that might be encountered in practical transmitters.

II. ANALYSIS

We consider a digital system with signaling interval (time slot) T. The data signal is assumed to be in the RZ format for launched pulses

of width $\alpha_l T < T$, and it merges into NRZ format when the launched pulses have width $\alpha_l T = T$ (i.e., $\alpha_l = 1$). The width $\alpha_l T$ of the pulse will be defined as the width of an isolated pulse (i.e., 010) launched into the fiber. The width of the output pulse from a dispersive fiber will be wider than $\alpha_l T$.

The model assumed in the analysis is shown in Fig. 1. A rectangular light pulse $h_l(t)$ of width $\alpha_l T$ with unity area is launched into a section of optical fiber and detected either by a thermal-noise-limited receiver or by a shot-noise-limited receiver. The output of the receiver amplifier is filtered and its output voltage $v_{out}(t)$ is presented to a decider circuit where the digital 1/0 decision is made. In the most general form, $v_{out}(t)$ can be calculated by use of

$$V_{out}(\omega) = kH_l(\omega) \cdot H_{fiber}(\omega) \cdot H_{filter}(\omega), \tag{1}$$

where $V_{out}(\omega)$ and $H_l(\omega)$ are the Fourier transforms of $v_{out}(t)$ and $h_l(t)$, respectively, and $H_{fiber}(\omega)$ and $H_{filter}(\omega)$ are the transfer functions of the fiber and the filter, respectively. The constant k depends on the quantum efficiency of the detector and gain of the amplifier, and it will be taken as unity in this analysis. The filter transfer function $H_{filter}(\omega)$ will be chosen as follows. In the absence of fiber dispersion and when the launched pulse has a specific width $\alpha_{l0}T$, we will choose the filter design so that $v_{out}(t)$ belongs to the "raised cosine" family[1] with the parameter $\beta = 1$. This output voltage, in the absence of fiber dispersion, will be denoted as $V_{out,\sigma=0}(\omega)$. It has the property that, in the time domain, its maximum value is at the center of its time slot and is zero at the center of all adjacent time slots, thus avoiding ISI. Then the filter function can be expressed as

$$H_{filter}(\omega) = \frac{V_{out,\sigma=0}(\omega)}{H_{l0}(\omega)} = \frac{(T/2)[1 + \cos(\omega T/2)]}{[\sin(\alpha_{l0}\omega T/2)/(\alpha_{l0}\omega T/2)]}, \qquad |\omega| T \leq 2\pi. \tag{2}$$

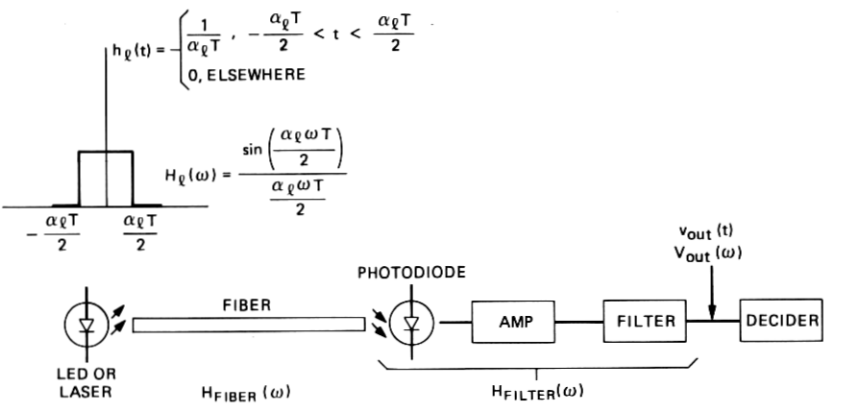

Fig. 1—Model of an optical fiber system.

As the launched-pulse width deviates from $\alpha_{l0}T$ and/or the fiber dispersion becomes nonzero, $V_{out}(\omega)$ deviates from $V_{out,\sigma=0}(\omega)$, and ISI arises. The fiber dispersion is assumed to be Gaussian and has the form

$$H_{fiber}(\omega) = \exp\{-\tfrac{1}{2}(\sigma_f\omega)^2\}, \tag{3}$$

where σ_f is the rms impulse response of the length of fiber used. Then, for any arbitrary rectangular input pulse of width $\alpha_l T$, the output pulse $v_{out}(t)$ can be calculated by inserting

$$H_l(\omega) = \frac{\sin(\alpha_l\omega T/2)}{\alpha_l\omega T/2},$$

$H_{filter}(\omega)$ from eq. (2), and $H_{fiber}(\omega)$ from eq. (3) into eq. (1), and then taking its inverse Fourier transform. Figure 2 shows the computed $v_{out}(t)$ for $\alpha_l = 0.3$ and 0.5 where $\sigma_f/T = 0$, and for $\alpha_l = 1.0$ where $\sigma_f/T = 0$, 0.2, and 0.4. For these computations the filter function was chosen to satisfy eq. (2) with $\alpha_{l0} = 1.0$. Note from Fig. 2 that $v_{out}(t)$ is nonzero

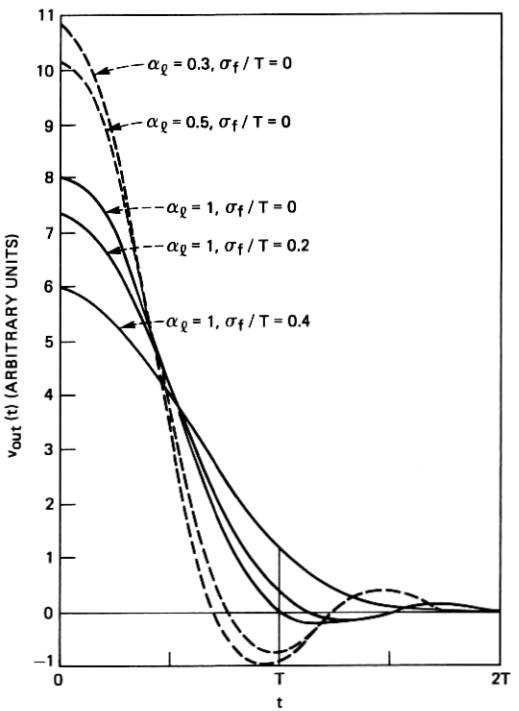

Fig. 2—Output waveform of an isolated pulse at the output of the filter for various pulse widths $\alpha_l T$ and fiber dispersion σ_f/T. The filter was set for a raised cosine output ($\beta = 1$) when $\alpha_{l0} = 1$ and $\sigma_f = 0$.

at the center of the neighboring time slot $t = T$ when $\alpha_l \neq 1$ and/or when $\sigma_f/T \neq 0$, resulting in ISI.

The sensitivity penalty caused by ISI can be calculated as follows. Let v_1 and v_2 be the values of $v_{out}(t)$ at the sampling time $t = 0$ (center of the time slot), for the cases where the pulse is on ("1" transmitted) and off ("0" transmitted), respectively. Levels v_1 and v_2 include contributions from adjacent pulses. The effect of such contributions is to decrease the difference between v_1 and v_2 compared with the ideal case [$\alpha_l = \alpha_{l0}$ and $(\sigma_f/T) = 0$]. We assume that the threshold decision level v_d is set for equal error probability P_e for both 1 and 0 pulses, then

$$\frac{v_1 - v_d}{v_{n1}} = \frac{v_d - v_2}{v_{n2}} = Q \tag{4}$$

and $P_e = (\frac{1}{2})\text{erfc}(Q/\sqrt{2})$, where v_{n1} and v_{n2} are the rms noise voltages when the pulse is on and off, respectively, and erfc denotes the complementary error function. Equation (4) can be rewritten as

$$v_1 - v_2 = (v_{n1} + v_{n2}) \cdot Q, \tag{5}$$

where $v_1 - v_2$ is referred to as the "eye opening."

In an ideal system, the eye opening is simply equal to the peak value of $v_{out}(t)$, and it will be denoted as v_1'. For systems with ISI, the appendix shows that the minimum $v_1 - v_2$ (i.e., the worst case eye opening) is

$$(v_1 - v_2)_{min} = v_{out}(0) - 2\,|\,v_{out}(T)\,|, \tag{6}$$

where $v_{out}(0)$ and $v_{out}(T)$ are the amplitudes of $v_{out}(t)$ at the centers of the time slot and the next adjacent time slot, respectively, when a 1 is transmitted.

The sensitivity penalty due to eye degradation can be expressed in terms of v_1' and $(v_1 - v_2)_{min}$. We have chosen two specific cases: (*i*) a thermal-noise-limited receiver which corresponds to a thermal-noise-limited amplifier with a pin photodiode or an avalanche photodiode (APD) operated at low gain, and (*ii*) a shot-noise-limited receiver which corresponds to a system with an APD operated at high gain.

2.1 Thermal-noise-limited case

Here, the shot noise due to the signal itself is negligible. In order to restore the degraded eye opening and achieve the same BER, the average received power has to be increased by an amount equal to the sensitivity penalty. The averge-power sensitivity penalty Θ_a is given by

$$\Theta_a = v_1'/(v_1 - v_2)_{min}, \tag{7}$$

where $(v_1 - v_2)_{min}$ can be calculated from eq. (6). The peak-power

sensitivity penalty Θ_p can be written as

$$\Theta_p = \Theta_a/\alpha_l. \tag{8}$$

Results from such calculations for various launched-pulse widths and fiber dispersions are shown as solid curves in Figs. 3a and 3b, where we assumed $\alpha_{l0} = 1$ in calculating the filter transfer function.

Note from Fig. 3a that, for small fiber dispersion (say, $\sigma_f/T \lesssim 0.2$), the average-power sensitivity penalty Θ_a is almost independent of

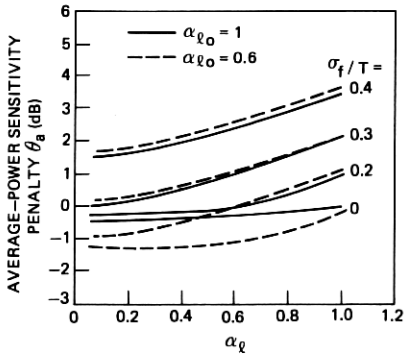

(a)

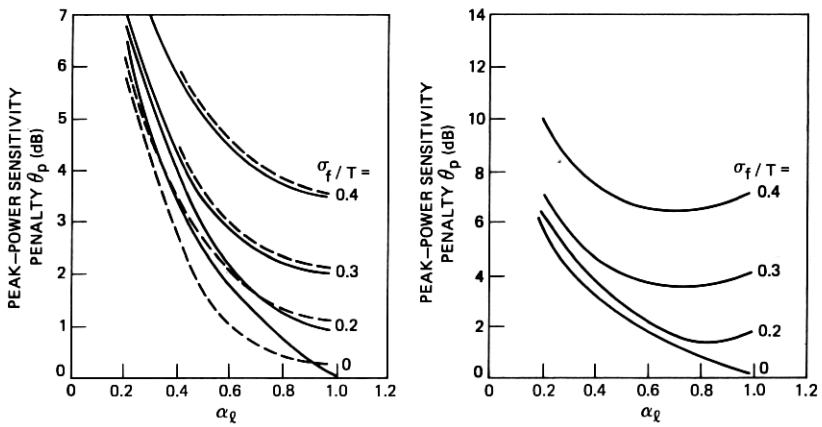

(b) (c)

Fig. 3—(a) Calculated average-power sensitivity penalties versus normalized pulse width α_l for various σ_f/T for the thermal-noise-limited case. Solid lines are for $\alpha_{l0} = 1$ and broken lines are for $\alpha_{l0} = 0.6$. Zero dB sensitivity penalty is at $\alpha_l = \alpha_{l0} = 1$ and $\sigma_f = 0$. Data pattern was in RZ format for $\alpha_l < 1$ and NRZ for $\alpha_l \geq 1$ in (a) to (c). (b) Calculated peak-power sensitivity penalties versus α_l for the thermal-noise-limited case. (c) Calculated peak-power sensitivity penalties versus α_l for the shot-noise-limited case. $\alpha_{l0} = 1$.

launched-pulse width $\alpha_l T$. That is, the receiver sensitivity depends mostly on the number of launched photons per pulse and not on the pulse width in this range of σ_f/T. Since the peak-power sensitivity penalty Θ_p is inversely proportional to α_l, Θ_p increases with reduced pulse width as shown in Fig. 3b. Thus, if the light emitter is peak-power limited, then wider launched pulses would be advantageous for the system with small fiber dispersion since the average-power emitted could be increased to permit greater fiber lengths. As the dispersion of the fiber becomes significant, one can intuitively understand that to minimize ISI, the launched-pulse width should be narrowed so that the effect of pulse-broadening by the fiber is partially compensated. This agrees with the results of the analysis, as one can see from Fig. 3a where Θ_a decreases as α_l becomes smaller. That is, if the fiber dispersion is significant, the number of photons per pulse required to attain a given BER decreases as the launched pulse width is reduced.

It has been previously shown[4] that the receiver sensitivity can be improved if the filter is set such that its output voltage is of the raised cosine form $V_{\text{out},\sigma=0}(\omega)$, as shown in eq. (2), when a reduced-width rectangular pulse (instead of a full-width pulse) impinges on the photodetector, because the noise bandwidth of such a filter will be narrower. That is, the receiver sensitivity improves if the filter were designed for minimum ISI with smaller α_{l0}, provided that the launched-pulse width $\alpha_l T$ is equal to $\alpha_{l0} T$ and the fiber dispersion is absent. As the width of the received pulses deviates from $\alpha_{l0} T$, ISI may arise and the receiver sensitivity may be degraded. We will compare the receiver sensitivity of two filter designs, one with $\alpha_{l0} = 1$ and the other with $\alpha_{l0} = 0.6$, as the launched-pulse widths deviate from $\alpha_{l0} T$ and as the fiber dispersion is increased. We also show that the minimum optical power required to achieve a given BER is proportional to $(I_2 I_3)^{1/4}$ for a thermal-noise-limited bipolar amplifier,[4] where I_2 and I_3 are the integrals defined by Personick in Ref. 1. The integrals are evaluated for $\alpha_{l0} = 0.6$ and the raised cosine form of filter output $V_{\text{out},\sigma=0}(\omega)$. Then, after repeating similar calculations for the sensitivity penalties previously described, Θ_a and Θ_p for $\alpha_{l0} = 0.6$ are shown as broken lines in Figs. 3a and 3b, respectively.

From Fig. 3a we see that, for $\sigma_f/T = 0$ and the pulse width less than $0.6T$, the average-power sensitivity penalty for a receiver with $\alpha_{l0} = 0.6$ is about 1 dB less than that of a receiver with $\alpha_{l0} = 1.0$. As the received pulse width widens, either because of the increased launched-pulse width and/or increased-fiber dispersion, the averge- and peak-power sensitivity penalties inflicted by ISI overshadow the small improvement in receiver sensitivity from the reduced noise bandwidth, and the difference in sensitivity penalties for $\alpha_{l0} = 1$ and $\alpha_{l0} = 0.6$ becomes negligible.

2.2 Shot-noise-limited case

In the shot-noise-limited case, the shot noise due to the signal dominates the thermal noise and the noise power is proportional to the optical power. Since the output-signal voltage v_1 is also proportional to the optical power, one can relate the noise voltage v_{n1} to v_1 as

$$v_{n1} = c(v_1)^{1/2}, \tag{9}$$

where c is a constant with a dimension of square root of voltage. With launched-pulse width $\alpha_l T$ equal to $\alpha_{l0} T$ and in the absence of fiber dispersion (i.e., no ISI), $v_1 = v_1'$, $v_2 = 0$, and $v_{n1} \gg v_{n2}$, then eq. (5) becomes

$$v_1 = v_1' \simeq v_{n1} Q. \tag{10}$$

As the input width deviates from $\alpha_{l0} T$ and/or as the fiber dispersion increases, the optical power has to be increased to compensate for the eye degradation, and also for the larger shot noise arising from the increased optical power itself. Thus, eq. (5) becomes

$$\Theta_a \cdot (v_1 - v_2)_{\min} \simeq v_{n1}' \cdot Q, \tag{11}$$

where $(v_1 - v_2)_{\min}$ is the degraded eye opening and v_{n1}' is the rms noise associated with the increased optical power. It can be expressed as

$$v_{n1}' = c \cdot (\Theta_a \cdot v_1)^{1/2}. \tag{12}$$

Substituting eqs. (9), (10), and (12) into eq. (11), we obtain

$$\Theta_a = \left\{ \frac{v_1'}{(v_1 - v_2)_{\min}} \right\}^2. \tag{13}$$

Thus, Θ_a in dB is twice the magnitude of Θ_a for the thermal-noise-limited case. The peak-power sensitivity penalty Θ_p is again related to Θ_a through eq. (8). With the data shown in Fig. 3a, Θ_p of the shot-noise-limited case was calculated, and it is shown in Fig. 3c for $\alpha_{l0} = 1$. Note that the minimum value of Θ_p occurs at progressively smaller α_l as σ_f/T increases. This is because Θ_a increases more rapidly for wider pulses as σ_f increases in this case, which in turn accentuates the increase in Θ_p.

III. EXPERIMENTS

We measured the average-power sensitivity penalties Θ_a as a function of launched-pulse width and fiber dispersion for a thermal-noise-limited receiver and for a receiver with equal thermal-noise and shot-noise levels. The rise and fall times of the launched pulses were less than 1 ns. To see the effect of slow rise and fall times on the sensitivity penalties, we increased each of these transition times to about 3 ns and then to about 8 ns, and the average-power sensitivity penalties

were measured for a thermal-noise-limited receiver. The peak-power sensitivity penalties Θ_p were then calculated from the measured Θ_a and the known pulse widths. As described in the previous section, the data signal was in RZ format for $\alpha_l < 1$ and it merged into NRZ format for $\alpha_l \geq 1$ for these sets of measurements. The normalized pulse width was extended beyond $\alpha_l = 1$ because the width of output light pulse from practical transmitters could be wider than the width of electrical pulse applied to the driver circuits. Note that the pulse width $\alpha_l T$ is defined as the width of an isolated pulse. When a data sequence with m consecutive 1 s occurs in the pseudo-random data signal, the transmitter output will be a sequence of m discrete pulses, each of width $\alpha_l T$ in the case of RZ format, and a single pulse of width $\alpha_l T + (m - 1)T$ in the case of NRZ format.

To simulate the effects of variation in pulse width, the data signal was then changed to NRZ format for $0.6 \leq \alpha_l \leq 1.4$, and the same measurements were repeated for the thermal-noise-limited receiver. When a data sequence with m consecutive 1 s occurs, the transmitter output will be a single pulse of width $\alpha_l T + (m - 1)T$ for the entire range of α_l in these measurements.

Light pulses of various widths from an injection laser ($\lambda = 0.83$ μm) or an LED ($\lambda = 0.89$ μm) modulated by a pseudo-random data signal at 45 Mb/s were launched into one of the strands of a seven-strand, 420-meter-long optical fiber cable. The fiber is a Ge-doped, graded-index fiber of NA $\simeq$ 0.33, core diameter $\simeq$ 50 μm, and cladding diameter $\simeq$ 110 μm. The fiber can be concatenated to various lengths up to 2.94 km. The dispersion of the fiber is measured by launching narrow optical pulses ($\simeq$ 1 ns from a laser and $\simeq$ 5 ns from an LED) into the fiber and detecting the broadened output pulses from the fiber with a high-speed avalanche photodetector. The detected pulses were generally slightly asymmetric about the peak, indicating that the transfer function of the fiber was not exactly Gaussian as was assumed in the analysis. Nevertheless, the full width between the points where the optical power was down by a factor of 0.6 from the peak power was taken as $2\sigma_f$, an approximation to the rms dispersion of a Gaussian transfer function in this experiment.

The receiver used was the 45 Mb/s regenerator designed for the Atlanta fiber-system experiment.[5] It used a Si avalanche photodetector (APD), a 4 kΩ transimpedance preamplifier, a main amplifier with automatic gain control, a low-pass filter, a decider circuit, and a phase-locked loop for timing recovery. The APD gain was fixed in these experiments at either 20 or 100. From previous measurements, this receiver was known to be thermal-noise-limited at an APD gain of 20, and to have a shot-noise level approximately equal to thermal noise at an APD gain of 100. The low-pass filter was designed to provide v_{out} ($\pm$ 22 ns) $\simeq$ 0 when the received pulse was a trapezoid with rise and

fall times of 3 ns and a width of 22 ns. Thus the filter design corresponds approximately to $\alpha_{l0} = 1$ of the analysis presented in the previous section. Error rates of the regenerated data were measured with a Tau-Tron bit-error-rate measurement system.

In the experiment, the launched light power was varied to maintain a BER of 10^{-6} as the pulse width was varied, and the dc current in the biasing circuit of the APD was recorded. This current is proportional to the average optical power impinging on the APD. The sensitivity penalty was taken as 0 dB when the launched-pulse width was 22 ns and the fiber dispersion $\sigma_f = 0$. The measured average-power sensitivity penalties Θ_a versus pulse width for various fiber length l are shown in Fig. 4a for the thermal-noise-limited case. The light source was an injection laser with optical rise and fall times less than 1 ns. The data signal was RZ for $\alpha_l < 1$, and NRZ for $\alpha_l \geq 1$. Θ_a taken from Fig. 3a are also shown as solid curves for comparison. Both the calculated and

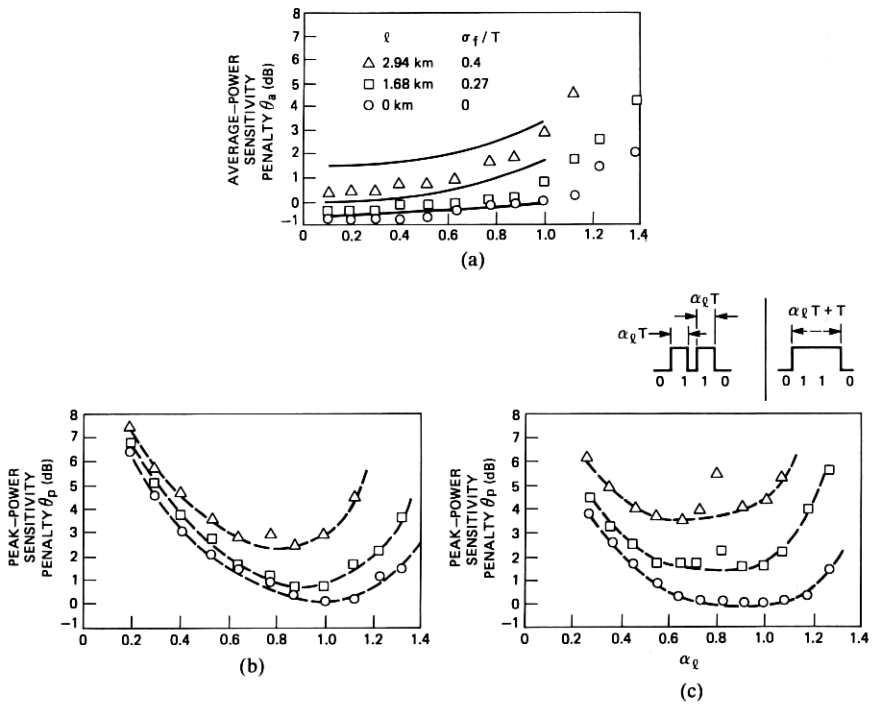

Fig. 4—(a) Measured average-power sensitivity penalties for the thermal-noise-limited case are shown as discrete points. The solid lines are the calculated values taken from Fig. 3a with $\alpha_{l0} = 1$. The rise and fall times of the launched pulses were approximately 1 ns, and data pattern was RZ for $\alpha_l < 1$ and NRZ for $\alpha_l \geq 1$ in (a)-(c). (b) Calculated peak-power sensitivity penalties deduced from the measured Θ_a for the thermal-noise-limited case. (c) Calculated peak-power sensitivity penalties deduced from the measured Θ_a for the receiver with approximately equal shot- and thermal-noise levels. The waveform of launched pulses for the pattern sequence 0110 is also shown.

measured Θ_a showed similar trends as a function of α_l and σ_f. Θ_a for reduced-width launched pulses were small even in the presence of a large fiber dispersion. However, they increased rapidly as the launched pulses widen beyond full width. In spite of the approximations used to simplify the analysis, the results of the measurements agreed reasonably well with the predictions.

To calculate Θ_p from the measured Θ_a, the contributions to changes in average photocurrent caused by changes in pulse width must be separated from those caused by changes in the peak optical power. Thus we separately measured the average photocurrent versus α_l, while the peak optical power was kept constant. From this measurement and the data shown in Fig. 4a, Θ_p was calculated and the results are shown in Fig. 4b. The broken lines in Fig. 4b (and also in Figs. 4c, 5, and 6) are simply joining most of the measured points. Note that a fairly broad minimum in Θ_p exists near $\alpha_l = 1$; that is, Θ_p is relatively insensitive to small changes in pulse width near $\alpha_l = 1$, as predicted theoretically.

Figure 4c shows Θ_p, inferred from the measured Θ_a for the case where the shot-noise and thermal-noise levels are approximately equal. Compared to the thermal-noise-limited case (Fig. 4b), one notices that Θ_p sensitivity penalties are larger, especially for $\alpha_l \geq 1$. Ignoring the anomalously large-power penalty near $\alpha_l = 0.8$ for the moment, one sees that the peak-power penalty has a broader minimum than the thermal-noise-limited case, and the minimum shifts toward smaller α_l as σ_f of the fiber increases. This tendency is in agreement with the calculation shown in Fig. 3c, where we assumed that the shot noise dominated the thermal noise. The anomaly at $\alpha_l = 0.8$ was due to the data-pattern-dependent magnitudes of v_{out}, where we observed that the magnitudes of isolated 1 s were smaller than the consecutive 1 s. This is because the receiver used in the experiments was designed for $\alpha_{l0} \simeq 1$ and, as a consequence, the isolated 1 s of reduced-width pulses do not have enough time to reach their peak magnitudes within the given time slot. The anomaly disappears for $\alpha_l \neq 0.8$, because, for $\alpha_l > 0.8$, pulses of even the isolated 1 s had enough time to reach their peak magnitudes, and for $\alpha_l < 0.8$, the distinction between the isolated and the consecutive 1 s disappeared (see insert of Fig. 4c). In practice, if the reduced-width launched pulses were to be used in the system, the low-pass filter would be redesigned to filter these reduced-width pulses to the raised cosine form, and the anomaly should not appear as α_l and σ_f are increased.

We then measured the added effects of slower rise and fall times of launched pulses on the receiver sensitivity, using an LED as a source. Figures 5a and 5b show the results expressed in terms of Θ_p, for the thermal-noise-limited case (APD gain = 20). The data signal is RZ for

$\alpha_l < 1$ and NRZ for $\alpha_l \geq 1$. The rise and fall times of the launched pulses are 3 ns and 4 ns, respectively, in Fig. 5a, and they are increased to 8 ns and 10 ns, respectively, in Fig. 5b. Since the pulse width is defined as the width between the midpoints of the leading and trailing edges, the area under the pulse (proportional to average optical power) is independent of rise and fall times. The average optical power required to achieve a given BER at zero-sensitivity penalty is independent of the rise and fall times of launched pulses; that is, the receiver sensitivities at zero penalty for the results shown in Figs. 4b, 5a, and 5b are the same. Except at the anomalous point near $\alpha_l = 0.8$, one notices that Θ_p versus α_l and σ_f are about equal (see Figs. 4b, 5a, and 5b). Thus we conclude that the receiver sensitivity is insensitive to the rise and fall times of launched pulses for up to approximately 10 ns in the 45 Mb/s system if σ_f/T is not larger than approximately 0.3.

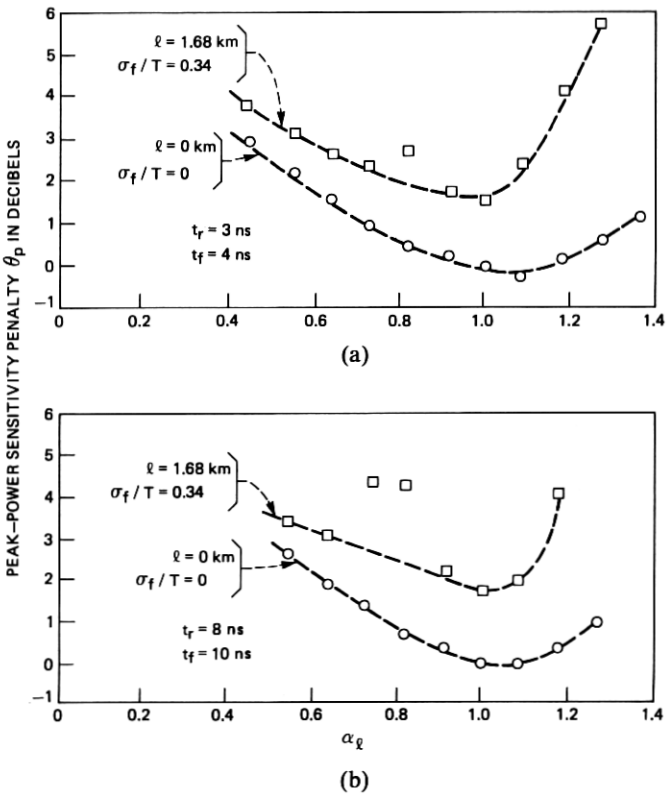

Fig. 5—Calculated peak-power sensitivity penalties obtained from measured Θ_a versus α_l for the thermal-noise-limited receiver, $\alpha_{l0} = 1$. (a) Rise and fall times of the launched pulses were 3 ns and 4 ns, respectively. (b) Rise and fall times of the launched pulses were 8 ns and 10 ns, respectively.

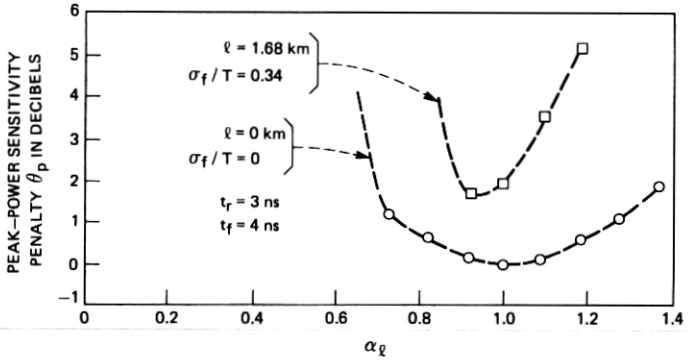

Fig. 6—Calculated peak-power sensitivity penalties obtained from measured Θ_a versus α_l for the thermal-noise-limited receiver. The data pattern was in NRZ format for the entire range of α_l. Rise and fall times of the launched pulses were 3 ns and 4 ns, respectively.

The transmitted signal from the LED was then changed to NRZ format for $0.6 \leq \alpha_l \leq 1.4$, and Θ_a versus pulse width was measured for the thermal-noise-limited case. The rise and fall times of launched pulses were 3 ns and 4 ns, respectively. Figure 6 shows the calculated Θ_p from the measured Θ_a versus α_l and σ_f. Note that Θ_p, for $\alpha_l \gtrsim 1$, are the same as those in Fig. 5a since the data signals are in NRZ format in both figures. However, the difference between the data from these figures becomes pronounced for $\alpha_l < 0.8$. In Fig. 5a, the anomalously large sensitivity penalty near $\sigma_l = 0.8$ disappears as α_l becomes smaller than 0.8, while it remains large even for $\alpha_l < 0.8$ in Fig. 6. The cause of the persistent anomaly is that the pulses for isolated and consecutive 1 s remain different in waveform in NRZ format for $\alpha_l < 0.8$. The anomalously large sensitivity penalty is due to the date-pattern dependent magnitude of v_{out}, as explained earlier.

IV. CONCLUSIONS

We have calculated and measured the average- and the peak-power sensitivity penalties inflicted on a lightwave receiver by intersymbol interference as a function of pulse width of the launched-data signal and of the fiber dispersion for nonequalizing receivers. We have also measured the sensitivity penalties versus pulse width, as the rise and fall times of launched pulses were increased.

We found that, for RZ format, the receiver sensitivity depended principally on the number of photons received per time slot and only weakly on the pulse shape (e.g., width, rise, and fall times) for reduced-width launched pulses and small fiber dispersion ($\sigma_f/T < 0.2$, say). As the pulse width increases beyond full width and/or as the fiber dispersion increases, the sensitivity penalties increase rapidly. However, even

in this region ($\alpha_l \lesssim 1.3$, $\sigma_f/T \lesssim 0.3$), the sensitivity penalties were relatively insensitive to rise and fall times of up to approximately 10 ns in the 45 Mb/s system. Thus, in the system where fiber dispersion is large, the reduced-width launched-pulse stream in RZ format has much less average-power sensitivity penalty Θ_a, caused by intersymbol interference. The peak-power sensitivity penalty Θ_p has a broad minimum near $\alpha_l = 1$ for the thermal-noise-limited receivers, and the minimum shifts toward smaller α_l for receivers with the shot-noise level either approaching or dominating the thermal-noise level. For example, the measured Θ_a decreased by 2.5 dB and the measured Θ_p by 1 dB, as the width of launched pulses was reduced from $1.1T$ to $0.6T$ when $\sigma_f/T = 0.4$ for the thermal-noise-limited receiver. For the receiver with equal shot-noise and thermal-noise levels, the measured Θ_a decreased by 4 dB and Θ_p by 2.5 dB for the corresponding change in pulse width and σ_f/T. We conclude that the sensitivity of nonequalized receivers improves by use of reduced-width launched pulses in RZ format (compared with the use of full-width launched pulses in NRZ format), particularly if the fiber dispersion is large. The optimum pulse width depends on the fiber dispersion and on whether the receiver is thermal-noise-limited or shot-noise-limited, and they can be found from Figs. 3a, 3b, and 3c. Similar conclusions were also given by Smith and Garrett for equalized receivers.[3] Since the peak-power sensitivity penalty has a broad minimum for $0.5 \lesssim \alpha_l \lesssim 1.0$, the use of reduced-width pulses in RZ format is also advantageous if the pulse width varies with temperature and/or varies among transmitters caused by product variations.

We have shown[4] that the receiver sensitivity improves if the filter is designed so that the reduced-width rectangular pulses, rather than the full-width pulses, are filtered to the raised-cosine form which goes through zero at the sampling times of neighboring bits. We have shown analytically that this improvement in sensitivity would be lost if the received pulses are broadened because of fiber dispersion and/or wider launched pulses.

V. ACKNOWLEDGMENTS

The authors wish to thank R. G. Smith, P. W. Shumate, and M. DiDomenico for their suggestions on the manuscript, G. Moy for his technical assistance, Lee Gusler for providing the optical regenerator, and P. Kaiser for providing the optical fiber cable.

APPENDIX

Worst-Case Eye Diagram

Consider the superposition of adjacent pulses for the following two cases.

(*i*) $v_{out}(T) < 0$ (Fig. 7a).

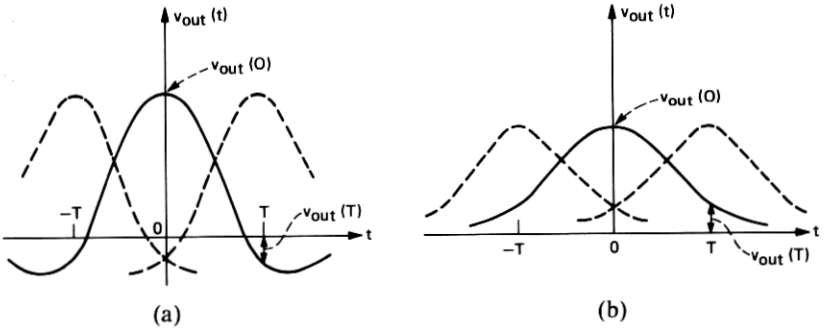

Fig. 7—$v_{out}(t)$ versus t. (a) $v_{out}(T) < 0$. (b) $v_{out}(T) > 0$.

The minimum $v_1(0)$ is obtained when pulses are present at $t = \pm T$. Then $v_1 = v_{out}(0) - 2\,|\,v_{out}(T)\,|$.

The maximum $v_2(0)$ is obtained when no pulses are present at $t = 0$ and $t = \pm T$. Then $v_2(0) = 0$. Thus $(v_1 - v_2)_{min} = v_{out}(0) - 2\,|\,v_{out}(T)\,|$.

(*ii*) $v_{out}(T) > 0$ (Fig. 7b).

The minimum v_1 is obtained when no pulses are present at $t = \pm T$. Then $v_1 = v_{out}(0)$. The maximum v_2 is obtained when pulses are present at $t = \pm T$. Then $v_2 = 2v_{out}(T)$. Thus $(v_1 - v_2)_{min} = v_{out}(0) - 2v_{out}(T)$.

REFERENCES

1. S. D. Personick, "Receiver Design for Digital Fiber Optic Communication Systems, I," B.S.T.J., *52* (July–Aug. 1973), pp. 843–886.
2. S. D. Personick, "Comparison of Equalizing and Unequalizing Repeaters for Optical Fiber Systems," B.S.T.J., *55* (Sept. 1976), pp. 957–971.
3. D. R. Smith and I. Garrett, "A Simplified Approach to Digital Optical Receiver Design," Opt. Quant. Electron., *10* (1978), pp. 211–221.
4. R. G. Smith and S. D. Personick, "Receiver Design for Fiber Communication Systems," in *Semiconductor Devices for Optical Communications*, H. Kressel, ed., New York: Springer, 1979, pp. 89–160.
5. T. L. Maione, D. D. Sell, and D. H. Wolaver, "Practical 45-Mb/s Regenerator for Lightwave Transmission," B.S.T.J., *57* (July–Aug. 1978), pp. 1837–1856.